

SUBARU SPECTROPOLARIMETRY OF MRK 573:  
THE HIDDEN HIGH-IONIZATION NUCLEAR EMISSION-LINE REGION  
INSIDE THE DUSTY TORUS<sup>a</sup>

<sup>a</sup>BASED ON DATA COLLECTED AT SUBARU TELESCOPE, WHICH IS OPERATED BY THE NATIONAL ASTRONOMICAL OBSERVATORY OF JAPAN.

TOHRU NAGAO<sup>2,3</sup>, KOJI S. KAWABATA<sup>4</sup>, TAKASHI MURAYAMA<sup>3</sup>, YOUICHI OHYAMA<sup>5</sup>,  
YOSHIAKI TANIGUCHI<sup>3</sup>, YASUHIRO SHIOYA<sup>3</sup>, RYOKO SUMIYA<sup>3</sup>, AND SHUNJI S. SASAKI<sup>3</sup>

<sup>2</sup> INAF – Osservatorio Astrofisico di Arcetri, Largo Enrico Fermi 5, 50125 Firenze, Italy;  
tohru@arcetri.astro.it

<sup>3</sup> Astronomical Institute, Graduate School of Science, Tohoku University, Aramaki, Aoba, Sendai 980-8578,  
Japan

<sup>4</sup> Astrophysical Science Center, Hiroshima University, 1-3-1 Kagamiyama, Higashi-Hiroshima, Hiroshima  
739-8526, Japan

<sup>5</sup> Subaru Telescope, National Astronomical Observatory of Japan, 650 North A'ohoku Place, University  
Park, Hilo, HI 96720

*The Astronomical Journal, in press*

ABSTRACT

We report on the result of our high quality spectropolarimetric observation for the narrow-line region in a nearby Seyfert 2 galaxy, Mrk 573, by the Subaru Telescope. The polarized flux spectrum of Mrk 573 shows not only prominent scattered broad H $\alpha$  emission but also various narrow forbidden emission lines. We find that the measured polarization degree of the observed forbidden emission lines is positively correlated with the ionization potential of the corresponding ions and the critical density of the corresponding transitions. We discuss some possible origins of these correlations, and then we point out that the correlations are caused due to the obscuration of the stratified narrow-line region in Mrk 573 by the optically and geometrically thick dusty torus, just similar to the previous study on NGC 4258.

*Subject headings:* galaxies: active - galaxies: individual (Mrk 573) - galaxies: nuclei - galaxies: Seyfert  
- polarization

1. INTRODUCTION

Active galactic nuclei (AGNs) can be broadly classified into two types; type 1 AGNs and type 2 AGNs, based on the presence or absence of broad permitted emission lines in their spectra. This dichotomy can be understood as follows: because high-velocity photoionized clouds in broad-line regions (BLRs) is surrounded by optically thick, dusty torus, the BLR can be seen only when we see the AGN from a face-on view toward dusty tori but is hidden by the torus when we see that from an edge-on view. This scheme is called AGN unified model (see Antonucci 1993 for a review), which has been supported by various observational facts, e.g., the detection of hidden BLRs in some type 2 AGNs observed in the polarized light (e.g., Antonucci & Miller 1985; Miller & Goodrich 1990; Tran, Miller, & Kay 1992; Young et al. 1993; Tran, Cohen, & Goodrich 1995; Tran 1995; Young et al. 1996; Kay & Moran 1998; Barth, Filippenko, & Moran 1999a, 1999b; Tran, Cohen, & Villar-Martin 2000; Kishimoto et al. 2001; Tran 2001; Lumsden et al. 2001; Nagao et al. 2004). This unified model is now one of the most important frameworks of AGN studies.

Being different from the BLR emission, narrow forbidden and permitted emission lines are seen in spectra of both type 1 and type 2 AGNs. This suggests that narrow-line regions (NLRs) are located far from the nucleus and thus its visibility should not depend on the viewing angle toward dusty tori. Recent imaging observations by HST

indeed clarify the spatially extended feature of NLRs in the scale of  $\sim 10^{1-3}$  pc (e.g., Capetti et al. 1995; Schmitt & Kinney 1996; Capetti, Axon, & Macchetto 1997; Falcke, Wilson, & Simpson 1998; Ferruit et al. 1999; Schmitt et al. 2003). However, it has been recently recognized that high-ionization forbidden emission lines such as [Fe VII] and [Fe X], and high critical-density transitions such as [O III] $\lambda 4363$  are statistically stronger in type 1 AGNs than in type 2 AGNs (e.g., Murayama & Taniguchi 1998a; Schmitt 1998; Nagao, Taniguchi, & Murayama 2000; Nagao, Murayama, & Taniguchi 2001a, 2001b). Does this suggest the breakdown of the AGN unified model? Murayama & Taniguchi (1998b) showed that this observed differences can be understood in the framework of the unified model as follows: the highly-ionized dense gas clouds, which radiate [O III] $\lambda 4363$  and high-ionization lines selectively, are located near the nucleus where they can be hidden by the tori, as well as BLRs (see also Nagao et al. 2001a, 2001b). Since this “high-ionization nuclear emission-line region (HINER)” plays a crucial role to construct realistic multi-zone photoionization models for NLRs, it is very important to investigate the nature of this HINER component.

However, it is far from feasible to resolve such a small scale comparable to the inner radius of the tori ( $< 1$  pc; e.g., Taniguchi & Murayama 1998; see also Minezaki et al. 2004 and references therein for the inferred inner ra-

dius of the tori by the dust reverberation technique). This is the case where the spectropolarimetry can display its unique ability, as mentioned already by Goodrich (1992). Note that the spectropolarimetric study of NLRs has been scarcely carried out up to now though many spectropolarimetric studies have been performed for BLRs and the continuum emission. One of few exceptional AGNs whose NLR is extensively investigated in a spectropolarimetric manner is a LINER galaxy NGC 4258 (Barth et al. 1999c). This object exhibits the following three interesting aspects; (1) the polarization degrees of forbidden lines are positively correlated with critical densities and ionization potentials of the line transitions, (2) the forbidden-line widths are broader in the polarized spectrum than those in the total flux spectrum, and (3) the gas density traced by the line ratio of the [S II] doublet is higher when using the polarized spectrum than when using the total flux spectrum. These observational facts are perfectly consistent with the HINER hypothesis; that is, the above three results can be consistently explained by introducing relatively high velocity, high dense and highly ionized clouds, whose radiation contribute to the polarized spectrum significantly, in the innermost region of NLRs whose visibility depends on a viewing angle toward dusty tori. The same results are also obtained for a quasar-hosted ultraluminous infrared galaxy IRAS P09104+4109 (Tran et al. 2000). However unfortunately, NLRs in Seyfert galaxies, which are the most typical population of AGNs in the local

Universe, have not yet been investigated in such a spectropolarimetric manner.

Therefore, we have started the project to perform spectropolarimetric observations of NLRs in type 2 Seyfert galaxies by using the Subaru Telescope to explore the innermost of NLRs. Although many spectropolarimetric observations have been performed for type 2 Seyfert galaxies historically, their data quality is not high enough. This is because most of such previous studies aimed to search for scattered BLR emission, which can be detected more easily than the scattered components of weak forbidden lines. Since very high-quality spectropolarimetric data is required for our purpose, the large aperture size of the Subaru Telescope is absolutely necessary. In this paper, we present the initial result of our project on a Seyfert 2 galaxy, Mrk 573<sup>1</sup>.

## 2. OBSERVATION AND DATA REDUCTION

The details of observations and the data reduction procedure are basically described in Nagao et al. (2004). However, we briefly describe these issues below for the convenience of the readers.

The spectropolarimetric observation for Mrk 573 was carried out by using FOCAS, Faint Object Camera And Spectrograph (Kashikawa et al. 2002) on the 8.2m Subaru Telescope (Kaifu et al. 2000; Iye et al. 2004) at Mauna Kea, on 2003 October 5–6 (UT). All the observations were carried out through a polarimetric unit that consists of

<sup>1</sup>The heliocentric radial velocity of Mrk 573 is  $5156 \pm 90$  km s<sup>-1</sup> (Whittle et al. 1988), which gives a projected linear scale of  $0.33 h_{75}^{-1}$  kpc for 1 arcsec.

TABLE 1  
TOTAL FLUX, POLARIZED FLUX, AND THE POLARIZATION DEGREE OF FORBIDDEN EMISSION LINES

Line	Total Flux <sup>a</sup> (10 <sup>-15</sup> ergs s <sup>-1</sup> cm <sup>-2</sup> )	Polarized Flux <sup>b</sup> (10 <sup>-15</sup> ergs s <sup>-1</sup> cm <sup>-2</sup> )	Pol. Degree (%)
[O III]λ4959 <sup>c</sup>	108.011±0.517	1.161±0.007	1.1
[O III]λ5007 <sup>c</sup>	312.151±1.495	3.356±0.019	1.1
[Fe VII]λ6087	6.234±0.092	0.116±0.007	1.9
[O I]λ6300 <sup>c</sup>	7.490±0.113 <sup>e</sup>	0.102±0.006 <sup>f</sup>	<1.4
[O I]λ6364 <sup>c</sup>	2.389±0.038	} 0.118±0.008 <sup>g</sup> {	<1.4
[Fe X]λ6374	2.503±0.075		>3.4
[N II]λ6548 <sup>c</sup>	23.439±0.365	0.181±0.004	0.8
[N II]λ6583 <sup>c</sup>	69.145±1.077	0.533±0.012	0.8
[S II]λ6717 <sup>d</sup>	17.514±0.364	} 0.316±0.014	0.8
[S II]λ6731 <sup>d</sup>	20.844±0.408		
[Ar III]λ7136	7.309±0.223	0.043±0.004	0.6
[O II]λ7320 <sup>d</sup>	1.609±0.062	} 0.049±0.005	1.4
[O II]λ7330 <sup>d</sup>	2.012±0.069		

<sup>a</sup>Measured from the total flux spectrum corrected for the contamination of the starlight of the host galaxy by the manner described in the text.

<sup>b</sup>Measured from the polarized flux spectrum on which a 15 pixel smoothing is performed except for [N II]λλ6548,6583, which are taken from Nagao et al. (2004); see text.

<sup>c</sup>The flux ratios and the velocity separations of the doublets of [O III], [O I] and [N II] are fixed to be the theoretical values. Note that it is not the case for the [O I] doublet in the polarized flux spectrum (see text).

<sup>d</sup>The velocity separations of the doublets of [S II] and [O II] are *not* fixed to be the theoretical values.

<sup>e</sup>Excluding the contribution of the [S III]λ6312 emission.

<sup>f</sup>Including the contribution of the polarized [S III]λ6312 emission.

<sup>g</sup>Sum of the polarized [O I]λ6364 and [Fe X]λ6374 emission.

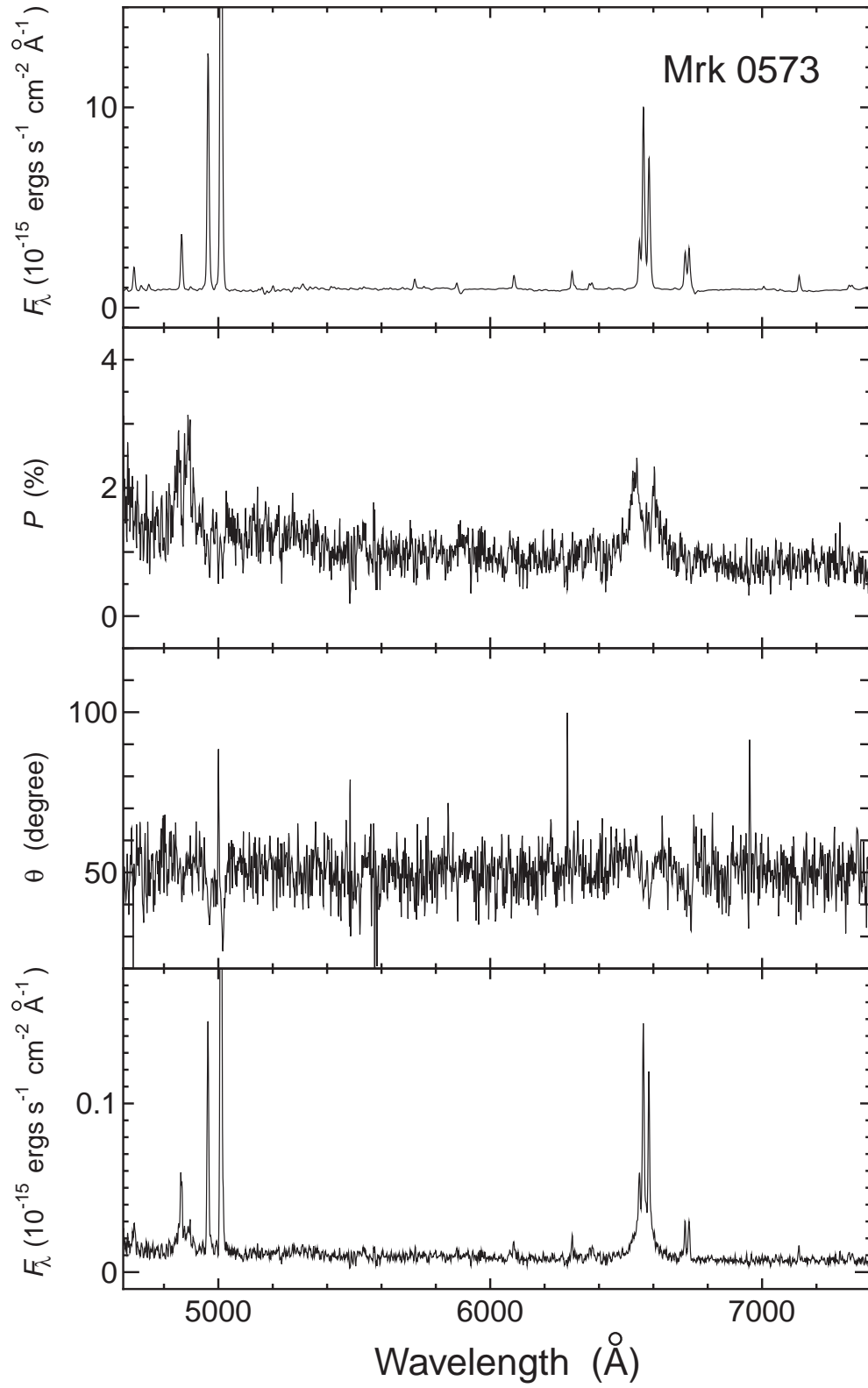


FIG. 1.— The obtained data of Mrk 573 are plotted as a function of wavelength. The data are corrected for the interstellar polarization and the redshift but not corrected for reddening and starlight of the host galaxy; (a) the total flux,  $I$ , (b) the polarization degree,  $P$ , (c) the position angle of polarization,  $\theta$ , and (d) the polarized flux (i.e.,  $I \times P$ ).

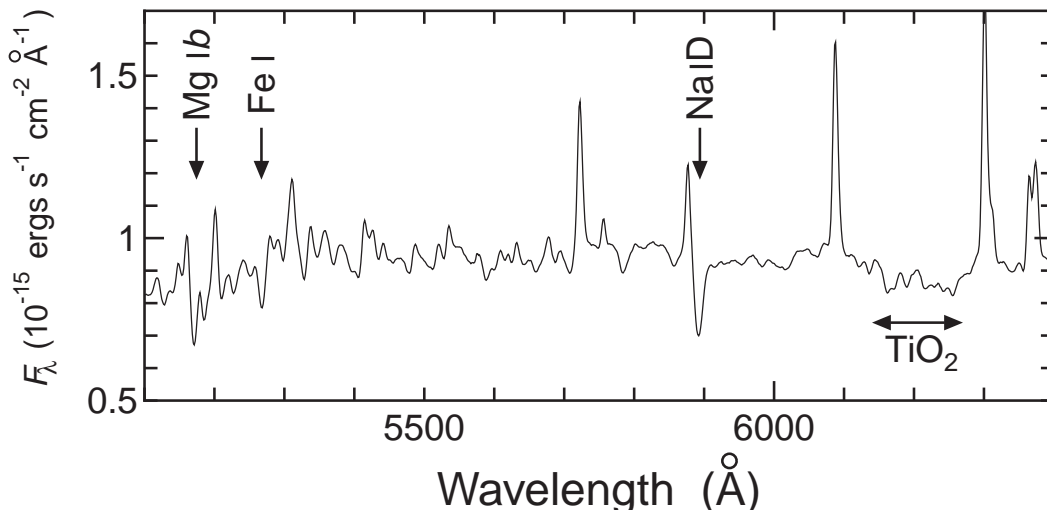


FIG. 2.— The enlarged total flux spectrum of Mrk 573. Note that the starlight contribution from the host galaxy is not corrected in this presented spectrum. Some significant spectral features of the starlight are identified.

a rotating superachromatic half-wave plate and a quartz Wollaston prism. A  $0''.4$  width slit, a 300 lines  $\text{mm}^{-1}$  gratings (300B), and an order-sorting filter of Y47 were used. This setting results in a wavelength resolution of  $R \sim 1000$ . We adopted a 3-pixel binning for the spatial direction on the chips, which results in the spatial sampling rate of  $0''.31$  for a binned pixel. All of the data were obtained at four wave-plate position angles,  $0.0^\circ$ ,  $45.0^\circ$ ,  $22.5^\circ$ , and  $67.5^\circ$ . The integration time of each exposure for the observation of Mrk 573 was 240 or 480 seconds, and the total on-source integration time was 208 minutes. The position angle of the slit was set to  $0^\circ$ . We also obtained spectra of unpolarized standard stars (BD+28° 4211 and G191B2B) and a strongly polarized star (HD 204827). Spectra of a halogen lamp and a thorium-argon lamp were also obtained for the flat fielding and the wavelength calibration, respectively.

The data were reduced by the standard manner, by using IRAF<sup>2</sup>. We extracted the spectra of Mrk 573 and the standard stars by adopting the aperture size of  $3''.1$  (i.e., 10 binned pixels). The corresponding linear aperture size in the frame of Mrk 573 is  $1.02 h_{75}^{-1} \text{ kpc} \times 0.13 h_{75}^{-1} \text{ kpc}$ . The instrumental polarization was corrected by using the data of the unpolarized standard stars. The instrumental depolarization was not corrected because it has been confirmed experimentally that the amount of the instrumental depolarization of the FOCAS is less than a few percent. The flux calibration was performed by using the data of BD+28° 4211 and G191B2B (Oke 1990). The polarization angle was calibrated by using the data of the strongly polarized star. The Galactic interstellar polarization toward the direction of Mrk 573 is estimated to be  $P = 0.32\%$  and  $\theta = 125^\circ$  at  $B$  band, based on the polarimetric properties of the two stars near the line of sight toward Mrk 573; i.e., HD 9740 and HD 10441 (see Table 1 of Nagao et al. 2004). Accordingly, the obtained spectrum was corrected for the Galactic interstellar polarization by adopting a Serkowski law (Serkowski, Mathewson, & Ford 1975) with  $P_{\text{max}}$  occurring at  $\lambda_{\text{max}} = 5500 \text{ \AA}$ .

### 3. RESULTS

The total flux ( $I$ ), the polarization degree ( $P$ ), the position angle of polarization ( $\theta$ ), and the polarized flux ( $I \times P$ ) of Mrk 573 are shown as functions of wavelength in Figure 1. The spectra shown in this figure are uncorrected for reddening and starlight of the host galaxy, but corrected for the redshift and the Galactic interstellar polarization as described in §2. The total flux spectrum of Mrk 573 is significantly contaminated with the starlight of the host galaxy; e.g., Kay (1994) reported that  $\sim 80\%$  of the continuum emission of Mrk 573 is attributed to the starlight at  $4400 \text{ \AA}$ . In order to display how the obtained total flux spectrum of Mrk 573 is contaminated with the starlight, we show the enlarged spectrum of the total flux in Figure 2. The strong stellar features such as Mg *Ib*  $\lambda 5177$ , Fe *I*  $\lambda 5270$ , Na *I* D  $\lambda 5893$ , and TiO<sub>2</sub> molecular band at  $\lambda 6235$  are clearly seen. Thus it should be kept in mind that the spectrum of the polarization degree shown in Figure 1b ( $P = 1.0 \pm 0.2\%$  at  $5400 - 6000 \text{ \AA}$ ; see Nagao et al. 2004) is heavily diluted by the unpolarized starlight emission.

As clearly exhibited in Figures 1b and 1d, a prominent broad component of the H $\alpha$  emission is detected in the spectrum of the polarized flux although there is no corresponding broad H $\alpha$  feature in the spectrum of the total flux (Figure 1a). We do not discuss this hidden-BLR emission in this paper, because this issue is discussed in the companion paper (Nagao et al. 2004) in detail. In addition to the broad emission lines, strong forbidden lines such as [O III]  $\lambda\lambda 4959, 5007$ , [N II]  $\lambda\lambda 6548, 6583$ , and [S II]  $\lambda\lambda 6717, 6731$  are clearly seen in the polarized flux spectrum and thus the polarization degree of such strong forbidden emission lines can be measured rather easily. However, being different from such strong forbidden emission lines, there are two difficulties to measure polarization degrees for rather weak but important forbidden lines.

One is the insufficient signal-to-noise ratio of the polarized flux spectrum. It is generally very difficult to obtain high quality spectra of polarized flux even by using 8m class telescopes, because it requires a huge number of pho-

<sup>2</sup>IRAF (Image Reduction and Analysis Facility) is distributed by the National Optical Astronomy Observatory, which is operated by the Association of Universities for Research in Astronomy Inc., under corporate agreement with the National Science Foundation.

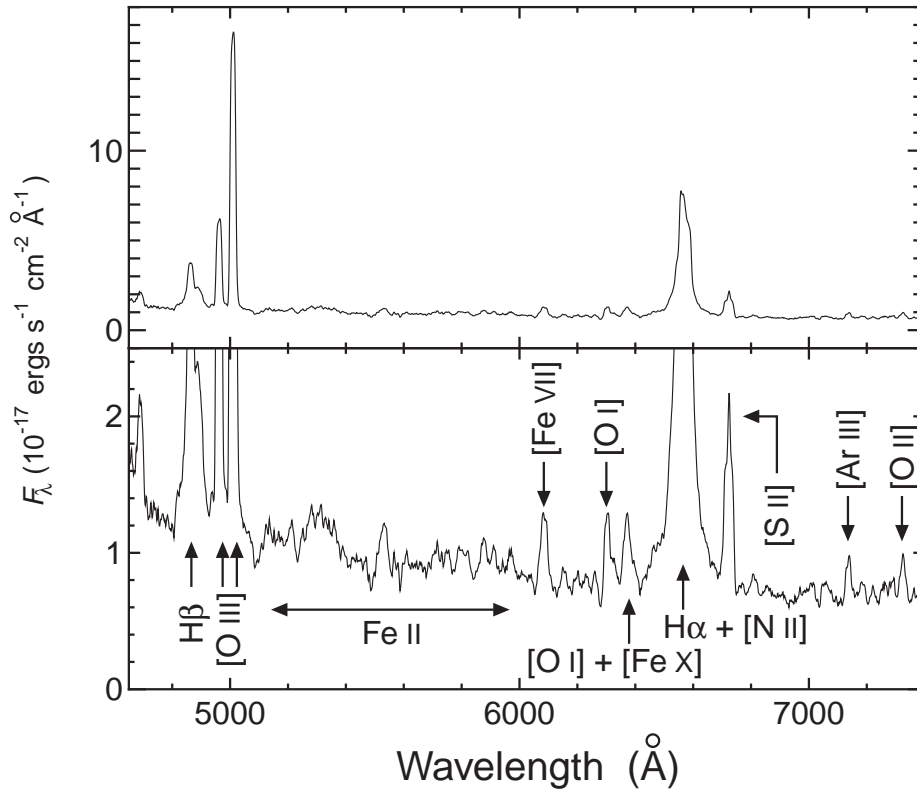


FIG. 3.— (*Upper*) The spectrum of the polarized flux. A 15 pixel smoothing is applied to improve the signal-to-ratio of the data. (*Lower*) Same as the upper panel, but the vertical scale is enlarged. Emission-line features in the polarized flux spectrum are identified.

tons. In order to improve this situation, we apply a 15 pixel (which corresponds to  $\approx 20.9 \text{ \AA}$ ) smoothing on the spectrum of the polarized flux. The resulting spectrum and its enlarged one are shown in Figure 3. This smoothed spectrum clearly shows various emission-line features including the Fe II multiplet, [Fe VII] $\lambda 6087$ , [Fe X] $\lambda 6374$ , [Ar III] $\lambda 7136$ , and [O II] $\lambda\lambda 7320, 7330$ . The [Fe X] $\lambda 6374$  emission line is blended with the [O I] $\lambda 6364$  emission in the smoothed spectrum. However, we can recognize that the [Fe X] $\lambda 6374$  emission is significantly polarized, because we can estimate the contribution of [O I] $\lambda 6364$  in the blended line by assuming the theoretical flux ratio of [O I] $\lambda 6300$ /[O I] $\lambda 6364 \approx 3.14$ . We can see that the strength of the blend of [O I] $\lambda 6364$  and [Fe X] $\lambda 6374$  is significantly stronger than one third of that of [O I] $\lambda 6300$  in the polarized flux spectrum as shown in Figure 3. The [O II] $\lambda\lambda 7320, 7330$  doublet is also blended in the smoothed spectrum of the polarized flux.

The other difficulty for the measurement of polarization degrees of weak emission lines is the contamination of the starlight from the host galaxy into the total flux spectrum. Since the continuum emission of the total flux of Mrk 573 is heavily contributed from the host galaxy as mentioned above (see also Kay 1994), the fluxes of weak emission lines are hard to be measured accurately owing to the complex spectral features of the starlight. Thus we should remove the starlight contribution in the total flux spectrum by using the model spectrum, in order to measure the fluxes of the weak emission lines in the total flux spectrum correctly. The stellar population of a host galaxy of AGNs are generally hard to be determined

accurately (see, e.g., Schmitt, Storchi-Bergmann, & Cid Fernandes 1999; Raimann et al. 2003). However, we are not interested in the accurate determination of the stellar population of the host galaxy of Mrk 573 but only interested in removing the stellar features roughly, in order to measure the polarization degrees of emission lines. We thus try to remove the stellar features by using only some template galaxy spectra.

As for the model spectrum, we adopt the simple stellar population (SSP) of Bruzual & Charlot (2003). We examine five SSPs as candidates of the representative stellar population of the host galaxy of Mrk 573; that is, (Age,  $Z$ ) = (5 Gyr,  $1.0 Z_{\odot}$ ), (10 Gyr,  $0.4 Z_{\odot}$ ), (10 Gyr,  $1.0 Z_{\odot}$ ), (10 Gyr,  $2.5 Z_{\odot}$ ), and (15 Gyr,  $1.0 Z_{\odot}$ ). Since the spectral resolution of the SSP spectra ( $\approx 2000$ ; see Bruzual & Charlot 2003) is not the same as that of the data obtained by our observation, we use the Gaussian kernel to match the spectral resolution of the models to the FOCAS data,  $R = 1000$ . The smoothed spectra of the five SSPs are shown in Figure 4. In order to judge which SSP is better as a template of the starlight of the host galaxy, we focus on two stellar absorption features; Na I D  $\lambda 5893$  and the TiO<sub>2</sub> molecular band at  $\approx 6235 \text{ \AA}$  (in the rest frame). Among the five SSPs, those with (Age,  $Z$ ) = (5 Gyr,  $1.0 Z_{\odot}$ ), (10 Gyr,  $0.4 Z_{\odot}$ ), and (10 Gyr,  $1.0 Z_{\odot}$ ) are not appropriate for the host galaxy spectrum. This is because the equivalent widths of Na I D  $\lambda 5893$  and the TiO<sub>2</sub> molecular band of these three SSPs are too small. In the remaining two SSPs, the one with (Age,  $Z$ ) = (10 Gyr,  $2.5 Z_{\odot}$ ) cannot eliminate the absorption features of Na I D  $\lambda 5893$  and the TiO<sub>2</sub> molecular band, simultane-

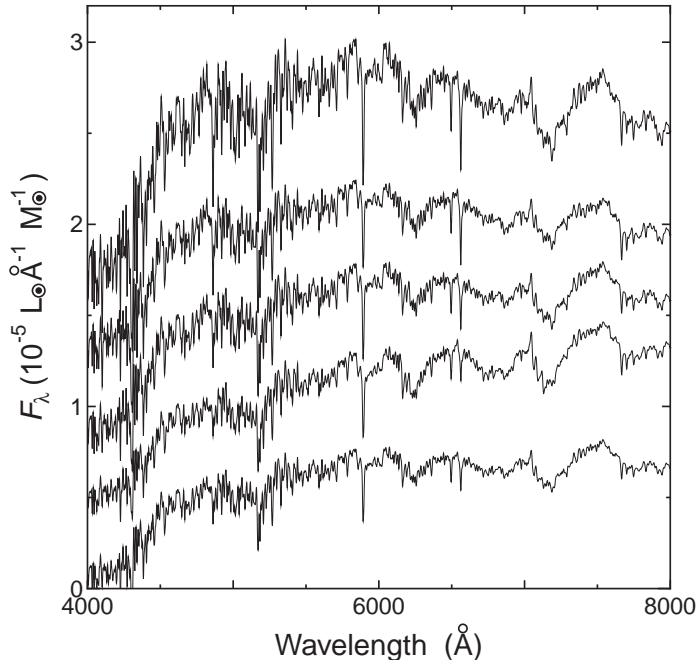


FIG. 4.— Spectra of five model SSPs of Bruzual & Charlot (2003) examined as a template of the host galaxy of Mrk 573 in our analysis. The spectra are smoothed to match the spectral resolution of our observational data,  $R = 1000$ . The adopted parameters for the SSPs are (Age,  $Z$ ) = (5 Gyr,  $1.0 Z_{\odot}$ ), (10 Gyr,  $0.4 Z_{\odot}$ ), (10 Gyr,  $1.0 Z_{\odot}$ ), (10 Gyr,  $2.5 Z_{\odot}$ ), and (15 Gyr,  $1.0 Z_{\odot}$ ), which are presented from top to bottom in the figure, respectively. The SSPs are displayed in unit of the solar luminosity per angstrom except for the model with (Age,  $Z$ ) = (15 Gyr,  $1.0 Z_{\odot}$ ), for which the constant of  $5 \times 10^{-6} L_{\odot} \text{\AA}^{-1}$  is subtracted for the presentation.

ously. We thus finally adopt the SSP with (Age,  $Z$ ) = (15 Gyr,  $1.0 Z_{\odot}$ ) as the template spectrum of the host galaxy of Mrk 573. The close-up views of the total flux spectra before and after the subtraction of the model galaxy spectrum are shown in Figure 5. The whole of the total flux spectrum after subtracting the starlight is shown in Figure 6. The fraction of the starlight of the host galaxy in the observed continuum spectrum of the total flux is  $\approx 84\%$  at  $\sim 5500 \text{\AA}$ , which is roughly consistent with the result of Kay (1994).

After these two treatments of the data to improve the measurement accuracy, we are now ready to measure the polarization degree of weak emission lines of Mrk 573. In the process of the measurements for the emission-line fluxes, we use the task SPECIFY in the IRAF, which was developed by Kriss (1994), assuming the Gaussian profile for the emission lines. We measure the unpolarized fluxes of the emission lines by using the total flux spectrum after removing the contribution of the starlight of the host galaxy. The flux ratios and the velocity separations of the doublets of [O III], [O I] and [N II] are fixed to be the theoretical values<sup>3</sup>. As for the doublets of [S II] and [O II], however, the velocity separations are not fixed to be the theoretical values, because the two emission lines in each doublet generally arise at different clouds in the NLR (see, e.g., Ferguson et al. 1997). For the measurement at the wavelength region around [O I] + [Fe X], we include the [S III] $\lambda 6312$  emission in the multi-Gaussian spectral modeling process because the [O I] $\lambda 6300$  emission is blended by that emission as seen in Figure 3. The measured flux ratio of [S III] $\lambda 6312$ /[O I] $\lambda 6300$  is  $\sim 0.26$ . As for the polarized

emission-line spectrum, the measurement is performed by using the polarized flux spectrum smoothed by 15 pixels except for the [N II] doublet, which cannot be measured in the smoothed spectrum due to the blending with the H $\alpha$  emission. For the [N II] flux, we thus refer the value presented in Nagao et al. (2004), in which no smoothing was performed for the polarized flux spectrum. The adjacent pairs of emission lines, [O I] $\lambda 6300$  plus [S III] $\lambda 6312$ , [O I] $\lambda 6363$  plus [Fe X] $\lambda 6374$ , [S II] $\lambda 6717$  plus [S II] $\lambda 6731$ , and [O II] $\lambda 7320$  plus [O II] $\lambda 7330$  cannot be deblended in the smoothed spectrum. Thus we adopt a single Gaussian profile for each pair, for the rough measurement of the sum of the emission-line fluxes.

The measured total flux and polarized flux, and the polarization degree for each forbidden emission line are given in Table 1. The derived polarization degree of the [O III] emission is higher than the previously reported value,  $0.27 \pm 0.09\%$  (Goodrich 1992). This may be due to the difference in the aperture size to make the one-dimensional spectra. Note that the slit width that we adopted is far narrower than that of the observation of Goodrich (1992),  $2''0$  arcsec. The upper-limited value of  $1.4\%$  for the polarization degree of [O I] $\lambda 6300$  is obtained by assuming that the [S III] $\lambda 6312$  emission is unpolarized. Under this assumption, we can estimate the polarized flux of the [Fe X] $\lambda 6374$  emission to be  $8.5 \times 10^{-17}$  ergs  $\text{s}^{-1} \text{cm}^{-2}$ , which corresponds to the polarization degree of  $3.4\%$ . On the other case, if the flux ratio of [S III] $\lambda 6312$ /[O I] $\lambda 6300$  in the polarized flux spectrum is the same as that in the total flux spectrum, the polarized flux of [O I] $\lambda 6300$  would be  $8.1 \times 10^{-17}$  ergs  $\text{s}^{-1} \text{cm}^{-2}$ . In this case, the polarization

<sup>3</sup>Here we adopt the flux ratios of 2.89, 0.319, and 2.95, and the wavelength ratios of 1.00967, 1.01007, and 1.00539, for the doublets of [O III] $\lambda\lambda 4959, 5007$ , [O I] $\lambda\lambda 6300, 6364$ , and [N II] $\lambda\lambda 6548, 6583$ , respectively (see, e.g., Osterbrock 1989).

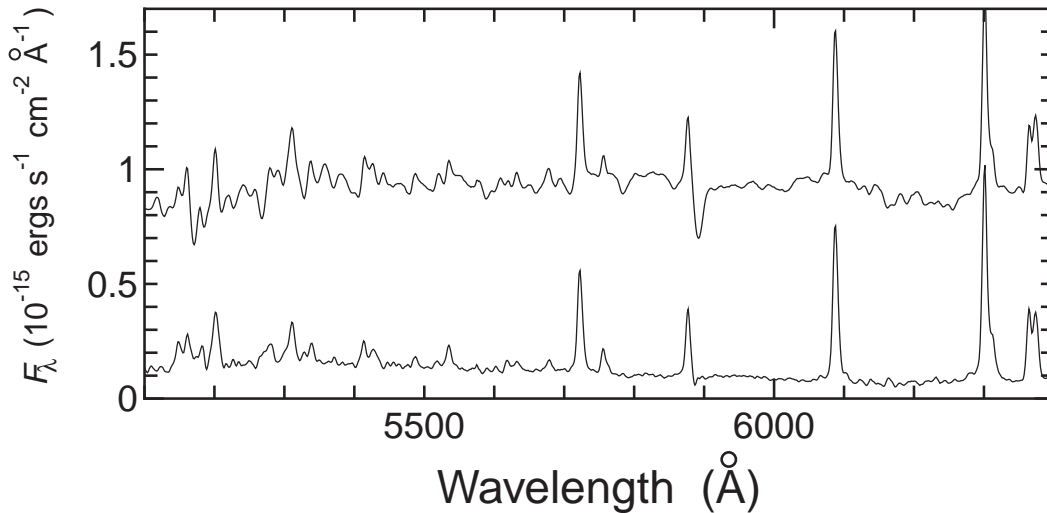


FIG. 5.— Close-up views of the total flux spectra before and after the subtraction of the model galaxy spectrum, i.e., the SSP of Bruzual & Charlot (2003) with (Age,  $Z$ ) = (15 Gyr, 1.0  $Z_{\odot}$ ).

degrees of [O I] and [Fe X] are estimated to be 1.1% and 3.7%, respectively.

#### 4. DISCUSSION

In order to interpret the obtained results, we plot the polarization degrees of the forbidden emission lines as functions of the ionization potential of corresponding ions and the critical density of corresponding transitions, in Figure 7. As shown in Figure 7, positive correlations are seen both between the polarization degree and the ionization potential and between the polarization degree and the critical density. Note that the typical error for the polarization degree is 0.1% at most, for faint emission lines. These correlations appear to be very similar to those seen in NGC 4258 (Barth et al. 1999c) and IRAS P09104+4109 (Tran et al. 2000). To investigate whether or not these positive correlations are statistically significant, we apply Spearman’s rank test where the null hypothesis is that the obtained polarization degree is not correlated with the ionization potential and with the critical density. The calculated probabilities that the data is consistent with the null hypothesis are 0.313 and 0.038 for the correlations of the polarization degree on the ionization potential and the critical densities respectively, in the case that the [S III] $\lambda$ 6312 emission is not polarized. As for the case that the polarization degree of the [S III] $\lambda$ 6312 emission is the same as the [O I] $\lambda$ 6300 emission, the probabilities are calculated to be 0.213 and 0.033, respectively. These results suggest that the correlation between the polarization degree and the ionization potential is statistically insignificant although that between the polarization degree and the critical density is statistically significant. This tendency seems to resemble the situation seen in NGC 4258 (see Figure 3 of Barth et al. 1999c). This result does not depend strongly on the assumption about the polarization property of the [S III] $\lambda$ 6312 emission. Note that if the [S III] $\lambda$ 6312 emission is more polarized than the [O I] $\lambda$ 6300 emission, the [O I] $\lambda$ 6300 and [Fe X] $\lambda$ 6374 polarization are correspondingly estimated to be < 1.1% and > 3.7%, respectively. Even in this case, the correlations seen in Figure 7 do not disappear. However, the [S III] $\lambda$ 6312 emission

may be not so strongly polarized because its critical density ( $\sim 1 \times 10^6 \text{ cm}^{-3}$ ) is lower than the critical density of the [O I] $\lambda$ 6300 emission ( $\sim 2 \times 10^6 \text{ cm}^{-3}$ ).

We then discuss the origin of the correlations. Sometimes NLR emission lines look to be polarized due to the Galactic interstellar polarization; i.e., narrow emission lines without intrinsic polarization can be seen in the polarized flux spectrum when the Galactic interstellar polarization is not corrected properly (e.g., Young et al. 1996). If the NLR polarization and its dependences on the ionization potential and the critical density are significantly attributed to the improper correction of the Galactic interstellar polarization, the polarization degree of the lines should be a function of the wavelength. Thus we plot the polarization degrees of the forbidden emission lines as a function of the line wavelength, in Figure 8. As shown in this figure, the polarization degree is not correlated with the line wavelength. This result strongly suggests that the observed NLR polarization and the correlations seen in Figure 7 are intrinsic, not due to the Galactic interstellar polarization. No clear correlation between the line flux and the polarization degree (Table 1) is also consistent with this idea.

The correlations may be created by the nuclear star-forming activity, because H II regions radiate lower ionization emission lines selectively than NLRs in AGNs. Since the emission from nuclear star-forming regions is thought to show a very small or no polarization, the observed polarization degree of lower-ionization emission lines may be more diluted by the nebular emission of the star-forming regions, than that of higher-ionization emission lines. And accordingly, the dependence of the dilution on the ionization potential of the forbidden lines could cause the observed correlations shown in Figure 7. However, this is not the probable scenario for Mrk 573. This is because the spectral properties of the host galaxy of Mrk 573 suggest that the stellar population of the host galaxy is very old and do not contain significant amount of young stars, which is suggested by the result of our SSP fitting (§3). González Delgado, Heckman, & Leitherer (2001) also reported that the stellar emission of Mrk 573 is dominated

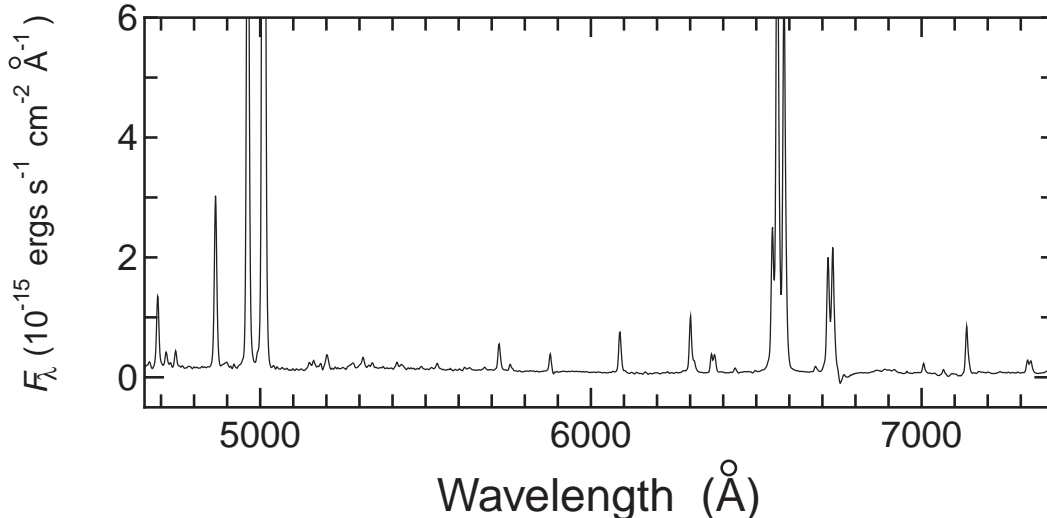


FIG. 6.— Total flux spectrum of Mrk 573 after subtracting the starlight contribution from the host galaxy, shown in the whole range of the spectral coverage.

by a old stellar population component, by a more quantitative manner than ours (see also Cid Fernandes et al. 2001; Raimann et al. 2003). Mouri & Taniguchi (2002) reported that the far-infrared emission of Mrk 573 is dominated by the AGN emission, not by the nuclear or circumnuclear starburst activity, which also supports the idea that the NLR emission of Mrk 573 is not diluted so significantly by the emission attributed by the star-forming activities.

A possible origin of the correlations inferred from the AGN unified model is that the highly ionized, dense part of NLRs (i.e., HINERs) is hidden by an edge-on, geometrically and optically thick torus. If the NLRs possess a stratified structure, highly ionized and/or high dense gas clouds should be more effectively hidden by the thick torus. In this case, emission lines with a higher ionization potential and/or a higher critical density can be seen in the polarized flux spectrum much more, which results in the positive correlations of the polarization degree of the forbidden emission lines with the ionization potential and the critical density. Since this scenario has been discussed for IRAS 20210+1121 (Young et al. 1996), NGC 4258 (Barth et al. 1999c), and IRAS P09104+4109 (Tran et al. 2000), it is very interesting to investigate whether or not this scenario is also the case for Mrk 573.

First, we focus on how significant the HINERs are hidden by the dusty torus in Mrk 573. Nagao et al. (2001a) demonstrated that the emission-line diagnostic diagram of  $[\text{O III}]\lambda 4363/[\text{O III}]\lambda 5007$  vs.  $[\text{Fe VII}]\lambda 6087/[\text{O III}]\lambda 5007$  is useful to examine the obscuration of HINERs (see Figure 12 of Nagao et al. 2001a). The optical spectrum of Mrk 573 shows only weak HINER emission ( $[\text{O III}]\lambda 4363/[\text{O III}]\lambda 5007 \sim 0.018$  and  $[\text{Fe VII}]\lambda 6087/[\text{O III}]\lambda 5007 \sim 0.013$ ; Nagao et al. 2000, 2001a), which is diagnosed that the HINER in Mrk 573 is very obscured compared to other Seyfert galaxies. Second, we refer to the previous literature about the spatially resolved observations of the NLRs. As for the HINER emission, Winge et al. (2000) presented by their near-infrared spectroscopy that the  $[\text{S IX}]1.252\mu\text{m}$  emission is unresolved although the neighboring  $[\text{Fe II}]1.257\mu\text{m}$  emission is clearly extended in Mrk 573. Low-ionization emission lines such as  $[\text{O III}]\lambda 5007$  are, on

the contrary, clearly extended around the central engine of Mrk 573 (e.g., Unger et al. 1987; Haniff, Wilson, & Ward 1988; Tsvetanov & Walsh 1992; Pogge & De Robertis 1995; Capetti et al. 1996; Schmitt et al. 2003). Since the polarization of the emission from this extended NLR is thought to be very small, the polarization degrees of low-ionization emission lines are diluted and thus the observed correlations can be created. Third, we check where the polarization of the NLR emission occurs in Mrk 573. It is known that the polarization angle of the nuclear continuum emission of type 2 AGNs tends to be perpendicular to the direction of extended NLRs and radio jets (e.g., Antonucci 1983; Brindle et al. 1990). This is attributed by the fact that the polarization is due to the scattering by free electrons in the opening cone above the torus. As for Mrk 573, the polarization angle of the nuclear continuum emission obeys the same tendency as the other type 2 AGNs (e.g., Nagao et al. 2004), which suggests that the observed polarization of the forbidden emission lines is also caused in the opening cone above the torus. Thus the scattering material can see the obscured HINER emission, which enables the HINER emission to be observed in the polarized flux spectrum.

If the polarization mechanism of the forbidden lines is the same as that of the broad permitted lines and the continuum emission, the position angle of the polarization of the forbidden lines should be similar to those of the broad lines and continuum emission. But, as expected from Figure 1c, the S/N of our data is not so sufficient to compare independently the position angles of the weaker forbidden lines, although some strong forbidden lines may show somewhat different position angles (Figure 1c). It should be thus examined by another deeper observation.

Taking all of the above matters into account, we conclude that the observed correlations presented in Figure 7 is caused due to the obscuration of the stratified NLR of Mrk 573 by the thick dusty torus, just similar to the previous studies on NGC 4258 and IRAS P09104+4109. This result is important as an evidence of the stratification of NLRs in AGNs. The velocity profiles of polarized forbidden emission lines are more useful to investigate this issue



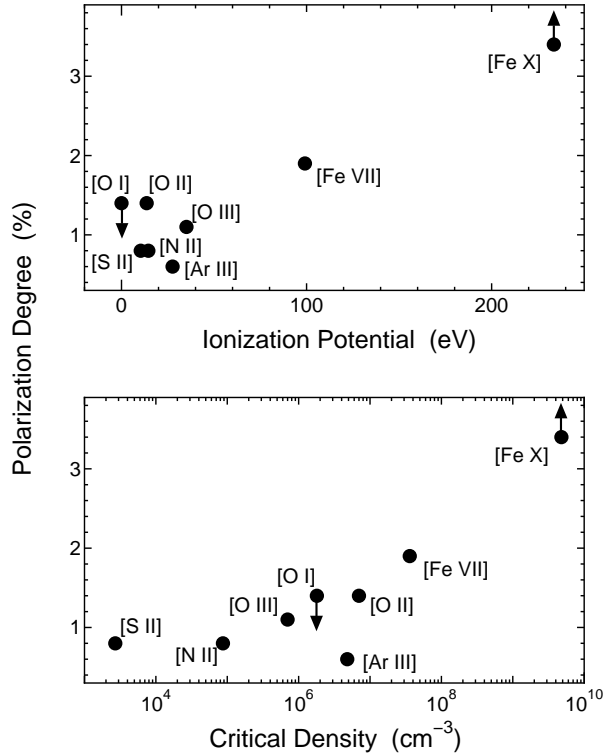


FIG. 7.— Polarization degrees of the forbidden emission lines as functions of the ionization potential of corresponding ions and the critical density of corresponding transitions. The polarization degrees of [O I] and [Fe X] are upper and lower limited values, respectively (see text).

further (Barth et al. 1999c), but the quality and the velocity resolution of our data are not high enough to carry out such an analysis.

Here we discuss the possibility that the correlations seen in Figure 7 are caused without any obscuration effect. If NLRs are stratified and thus HINERs reside in the innermost part of NLRs, photons arising at HINERs move longer optical path in the scatterer than the photons arising at the outer, low-ionization NLRs. The correlation of the polarization degree with the ionization potential and the critical density may be attributed to this difference. If this effect is the dominant source of the correlations seen in Figure 7 and the obscuration by the torus is not so important to create the correlations, the correlations should be discovered also in type-1 AGNs, just similar to type-2 AGNs such as Mrk 573 and NGC 4258. Further spectropolarimetry of NLRs in AGNs by 8m-class telescopes will bring us useful information about the structure of the innermost part of NLRs, which is never resolved spatially by current observational facilities.

Finally we remark that the measured polarization degrees of the forbidden emission lines,  $\sim 0.6\% - 3.4\%$ , are comparable to or larger than the polarization degree of the continuum emission ( $\sim 1.0\%$ ) although the nuclear continuum emission arise from more compact region than the NLR emission. This problem can be completely solved by remembering the dilution effect by the starlight of the host galaxy on the polarization degree of the continuum emission. We can correct the dilution effect by adopting the fraction of the starlight in the continuum emission. If we adopt 84% as a starlight fraction of

the continuum emission (see §3), the intrinsic polarization degree of the continuum emission is calculated to be  $1.0/(1 - 0.84) \sim 6.3\%$ , which is roughly consistent with the previous result of Kay (1994). This corrected polarization degree of the nuclear continuum emission is significantly larger than the polarization degrees of all forbidden emission lines. Note that the difference in the polarization degree between the NLR emission and the starlight-corrected continuum emission is due to the dilution effect by the unobscured part of the NLR. As mentioned above, some forbidden lines of Mrk 573 have been observed to be spatially extended (see, e.g., Unger et al. 1987; Haniff et al. 1988; Tsvetanov & Walsh 1992; Pogge & De Robertis 1995; Capetti et al. 1996; Schmitt et al. 2003). Emission-line imaging observations with a high quality and a high spatial resolution for higher ionization forbidden lines is important to interpret the polarization properties of the NLR emission further.

We are grateful to all the staffs of the Subaru telescope, especially to the FOCAS instrument team. We thank the referee, R. Goodrich, for his comments which improve this paper fruitfully. We also thank K. Matsuda and M. Seki for useful comments. TN acknowledges financial support from the Japan Society for the Promotion of Science (JSPS) through JSPS Research Fellowships for Young Scientists. A part of this work was financially supported by Grants-in-Aid for the Scientific Research (10044052, 10304013, and 13740122) of the Japanese Ministry of Education, Culture, Sports, Science, and Technology.

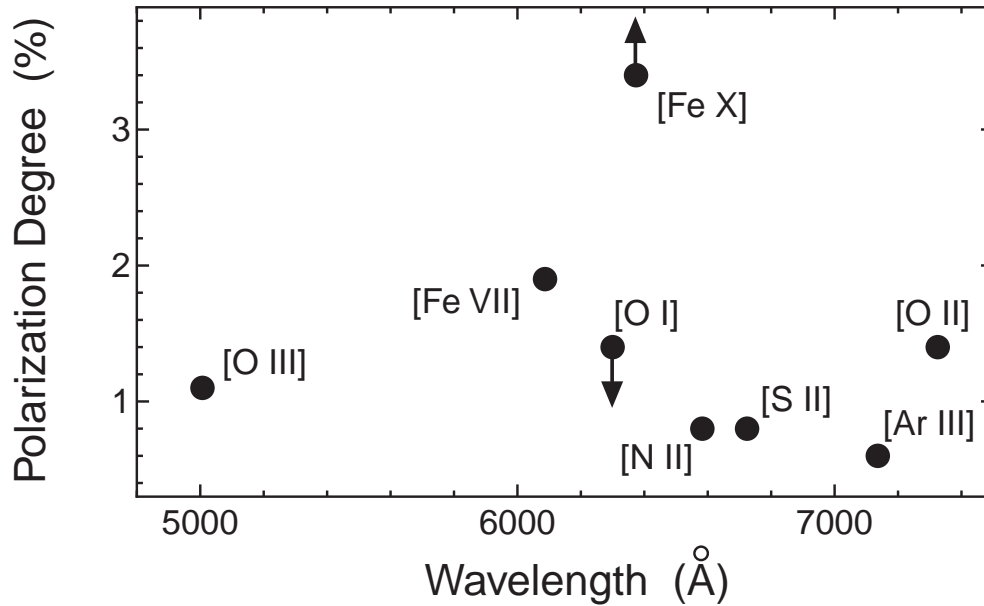


FIG. 8.— Polarization degrees of the forbidden emission lines as a function of the rest wavelength of the emission lines. The arrows are the same as those in Figure 7.

#### REFERENCES

- Antonucci, R. R. J. 1983, *Nature*, 303, 158  
Antonucci, R. R. J. 1993, *ARA&A*, 31, 473  
Antonucci, R. R. J., & Miller, J. S. 1985, *ApJ*, 297, 621  
Barth, A. J., Filippenko, A. V., & Moran, E. C. 1999a, *ApJ*, 515, L61  
Barth, A. J., Filippenko, A. V., & Moran, E. C. 1999b, *ApJ*, 525, 673  
Barth, A. J., Tran, H. D., Brotherton, M. S., Filippenko, A. V., Ho, L. C., van Breugel, W., Antonucci, R., & Goodrich, R. W. 1999c, *AJ*, 118, 1609  
Brindle, C., Hough, J. H., Bailey, J. A., Axon, D. J., Ward, M. J., Sparks, W. B., & McLean, I. S. 1990, *MNRAS*, 244, 577  
Bruzual, G., & Charlot, S. 2003, *MNRAS*, 344, 1000  
Capetti, A., Axon, D. J., & Macchetto, F. D. 1997, *ApJ*, 487, 560  
Capetti, A., Axon, D. J., Macchetto, F., Sparks, W. B., & Boksenberg, A. 1996, *ApJ*, 469, 554  
Capetti, A., Macchetto, F., Axon, D. J., Sparks, W. B., & Boksenberg, A. 1995, *ApJ*, 448, 600  
Cid Fernandes, R., Heckman, T., Schmitt, H., González Delgado, R. M., & Storchi-Bergmann, T. 2001, *ApJ*, 558, 81  
Falcke, H., Wilson, A. S., & Simpson, C. 1998, *ApJ*, 502, 199  
Ferguson, J. W., Korista, K. T., Baldwin, J. A., & Ferland, G. J. 1997, *ApJ*, 487, 122  
Ferruit, P., Wilson, A. S., Falcke, H., Simpson, C., Pécontal, E., & Durret, F. 1999, *MNRAS*, 309, 1  
González Delgado, R. M., Heckman, T., & Leitherer, C. 2001, *ApJ*, 546, 845  
Goodrich, R. W. 1992, *ApJ*, 399, 50  
Haniff, C. A., Wilson, A. S., & Ward, M. J. 1988, *ApJ*, 334, 104  
Iye, M., et al. 2004, *PASJ*, 56, 381  
Kaifu, N. et al. 2000, *PASJ*, 52, 1  
Kashikawa, N., et al. 2002, *PASJ*, 54, 819  
Kay, L. E. 1994, *ApJ*, 430, 196  
Kay, L. E., & Moran, E. C. 1998, *PASP*, 110, 1003  
Kishimoto, M., Antonucci, R. R. J., Cimatti, A., Hurt, T., Dey, A., van Breugel, W., & Spinrad, H. 2001, *ApJ*, 547, 667  
Kriss, G. A. 1994, *ASP Conf. Ser.*, 61, 437  
Lumsden, S. L., Heisler, C. A., Bailey, J. A., Hough, J. H., & Young, S. *MNRAS*, 2001, 327, 459  
Miller, J. S., & Goodrich, R. W. 1990, *ApJ*, 355, 456  
Minezaki, T., Yoshii, Y., Kobayashi, Y., Enya, K., Suganuma, M., Tomita, H., Aoki, T., & Peterson, B. A. 2004, *ApJ*, 600, L35  
Mouri, H., & Taniguchi, Y. 2002, *ApJ*, 565, 786  
Murayama, T., & Taniguchi, Y. 1998a, *ApJ*, 497, L9  
Murayama, T., & Taniguchi, Y. 1998b, *ApJ*, 503, L115  
Nagao, T., Kawabata, K. S., Murayama, T., Ohya, Y., Taniguchi, Y., Sumiya, R., & Sasaki, S. S. 2004, *AJ*, 128, 109  
Nagao, T., Murayama, T., Shioya, Y., & Taniguchi, Y. 2003, *AJ*, 126, 1167  
Nagao, T., Murayama, T., & Taniguchi, Y. 2001a, *ApJ*, 549, 155  
Nagao, T., Murayama, T., & Taniguchi, Y. 2001b, *PASJ*, 53, 629  
Nagao, T., Taniguchi, Y., & Murayama, T. 2000, *AJ*, 119, 2605  
Oke, J. B. 1990, *AJ*, 99, 1621  
Osterbrock, D. E. 1989, *Astrophysics of Gaseous Nebulae and Active Galactic Nuclei* (Mill Valley: University Science Books)  
Pogge, R. W., & De Robertis, M. M. 1995, *ApJ*, 451, 585  
Raimann, D., Storchi-Bergmann, T., González Delgado, R. M., Cid Fernandes, R., Heckman, T., Leitherer, C., & Schmitt, H. 2003, *MNRAS*, 339, 772  
Schmitt, H. R. 1998, *ApJ*, 506, 647  
Schmitt, H. R., Donley, J. L., Antonucci, R. R. J., Hutchings, J. B., & Kinney, A. L. 2003, *ApJS*, 148, 327  
Schmitt, H. R., Kinney, A. L. 1996, *ApJ*, 463, 498  
Schmitt, H. R., Storchi-Bergmann, T., & Cid Fernandes, R. 1999, *MNRAS*, 303, 173  
Serkowski, K., Mathewson, D. L., & Ford, V. L. 1975, *ApJ*, 196, 261  
Taniguchi, Y., & Murayama, T. 1998, *ApJ*, 501, L25  
Tran, H. D. 1995, *ApJ*, 440, 565  
Tran, H. D. 2001, *ApJ*, 554, L19  
Tran, H. D., Cohen, M. H., & Goodrich, R. W. 1995, *AJ*, 110, 2597  
Tran, H. D., Cohen, M. H., & Villar-Martin, M. 2000, *AJ*, 120, 562  
Tran, H. D., Miller, J. S., & Kay, L. E. 1992, *ApJ*, 397, 452  
Tsvetanov, Z., & Walsh, J. R. 1992, *ApJ*, 386, 485  
Unger, S. W., Pedlar, A., Axon, D. J., Whittle, M., Meurs, E. J. A., & Ward, M. J. 1987, *MNRAS*, 228, 671  
Whittle, M., Pedlar, A., Meurs, E. J. A., Unger, S. W., Axon, D. J., & Ward, M. J. 1988, *ApJ*, 326, 125  
Winge, C., Storchi-Bergmann, T., Ward, M. J., & Wilson, A. S. 2000, *MNRAS*, 316, 1  
Young, S., Hough, J. H., Bailey, J. A., Axon, D. J., & Ward, M. J. 1993, *MNRAS*, 260, L1  
Young, S., Hough, J. H., Efstathiou, A., Wills, B. J., Bailey, J. A., Ward, M. J., & Axon, D. J., 1996, *MNRAS*, 281, 1206